

**Efficient CO<sub>2</sub> fixation under atmospheric pressure using metal and halide-free heterogeneous catalyst**

Saikat Mandal<sup>#</sup>, Khushboo S. Paliwal<sup>#</sup>, Antarip Mitra<sup>#</sup>, and Venkataramanan Mahalingam\*

Department of Chemical Sciences, Indian Institute of Science Education and Research (IISER) Kolkata,

Mohanpur, West Bengal, 741246, India

E-mail: mvenkataramanan@yahoo.com

#These authors contributed equally

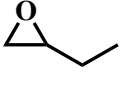
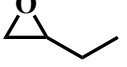
## Materials

Epichlorohydrin and other epoxides (TCI and Sigma Aldrich), 2,4,6-triamino pyrimidine (Merck), terephthaldehyde (Sigma Aldrich) and organic solvents DMF, methanol and acetone (Merck), NMR solvents,  $\text{CDCl}_3$  (Sigma Aldrich) are used as obtained.

## Instrumentation

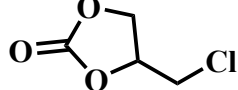
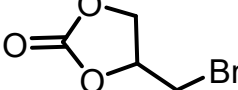
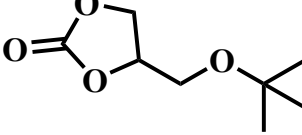
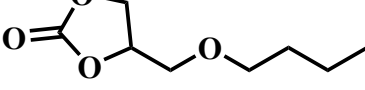
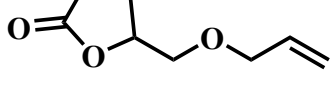
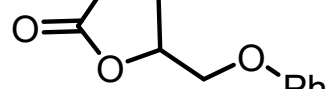
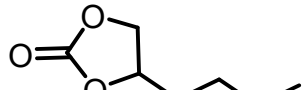
PXRD measurements are carried out in a Rigaku MiniFlex600 diffractometer attached with a D/tex ultradetector and Cu  $\text{K}\alpha$  source operating at 15 mA and 40 kV. FT-IR measurements are performed in a Perkin Elmer Spectrum instrument. Field emission SEM images and EDS are acquired on a SUPRA 55-VP instrument with patented GEMINI column technology. Prior to measurements, the samples are coated with a thin layer of gold-palladium to avoid charging effects. The TEM images and EDS are collected on a JEM 2100F field emission transmission electron microscope operating at 200 kV.  $^1\text{H}$  spectra are recorded on a Bruker AVANCE Ultrashield Plus 500 MHz spectrometer.

**Table S1.** Reaction of Propylene oxide and Butylene oxide with  $\text{CO}_2$

Epoxide	Temperature of reaction	Time	Conversion
 (B.P. 34 °C)	Room temperature	24 h	No conversion
 B.P. 65 °C	Room temperature	24 h	No conversion
	60 °C	24 h	>10%

**Conditions:** epoxide (15 mmol); POP (100 mg);  $\text{P}_{\text{CO}_2}$  (1 atm, balloon).

**Table S2.** Isolated yield of four synthesized cyclic carbonates

Cyclic Carbonate	Weight of Product (mg)	Weight Obtained (mg)	Isolated yield (%)
	2039	1632	80 %
	2699	2537	94 %
	2613	1959	75 %
	2613	2195	84 %
	2370	1967	83 %
	2910	2183	75 %
	2161	1729	80 %

**Conditions:** epoxide (15 mmol); POP (100 mg); P<sub>CO<sub>2</sub></sub> (1 atm, balloon); time (24 h).

**Table S3-** Comparison of the catalytic activity of different materials which are active for CO<sub>2</sub> fixation with epoxides under metal-free and halide-free conditions

Entry	Catalyst	Pressure (MPa)	Temp (°C)	Time (h)	Nature	Reference
1	Covalent triazine frameworks	1 MPa	130	4	Heterogeneous	S1
2	Bio-based organic polyamides	1 MPa	110	25	Heterogeneous	S2
3	Polyurethane	9 MPa	150	16	Heterogeneous	S3
4	Covalent triazine frameworks 2	0.69 MPa	130	4	Heterogeneous	S4
5	TBD@Merrifield	0.5 MPa	70	18	Heterogeneous	S5
6	Triazine-based nanoporous polymer	0.4 MPa	100	20	Heterogeneous	S6
7	PyridylSalicylimines	0.1 MPa	100	24	Heterogeneous	S7
8	4-aminopyridines	0.1 MPa	100	24	Heterogeneous	S8
9	Zn-adenine MOF	0.1 MPa	100	24	Heterogeneous	S9
10	Al-PDC (co-ordination polymer)	0.1 MPa	100	20	Heterogeneous	S10
11	α-AlOOH	0.1 MPa	100	24	Heterogeneous	S11
<b>12</b>	<b>Porous organic polymer (POP)</b>	<b>0.1 MPa</b>	<b>105</b>	<b>24</b>	<b>Heterogeneous</b>	<b>This work</b>

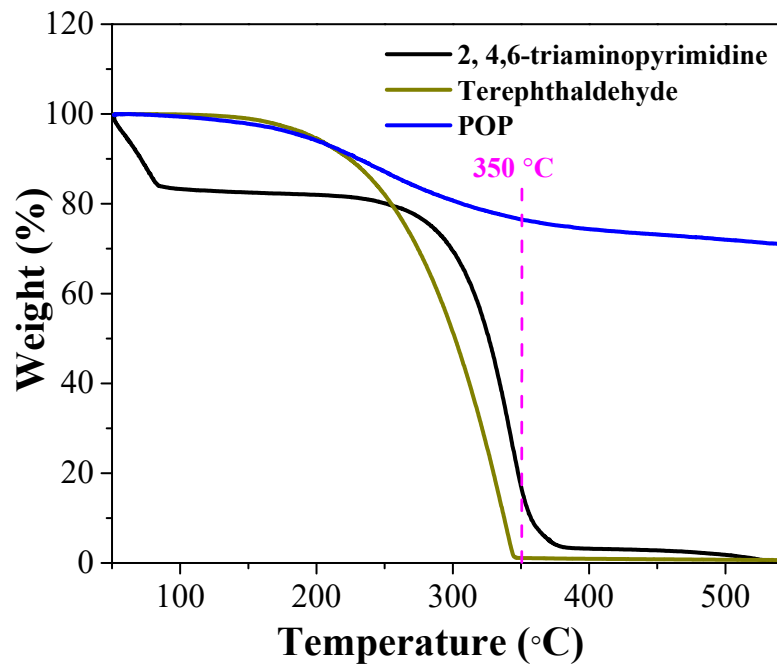


**Figure S1-** Thermogravimetric analysis (TGA) plots of 2,4,6-triaminopyrimidine, terephthaldehyde, and POP.

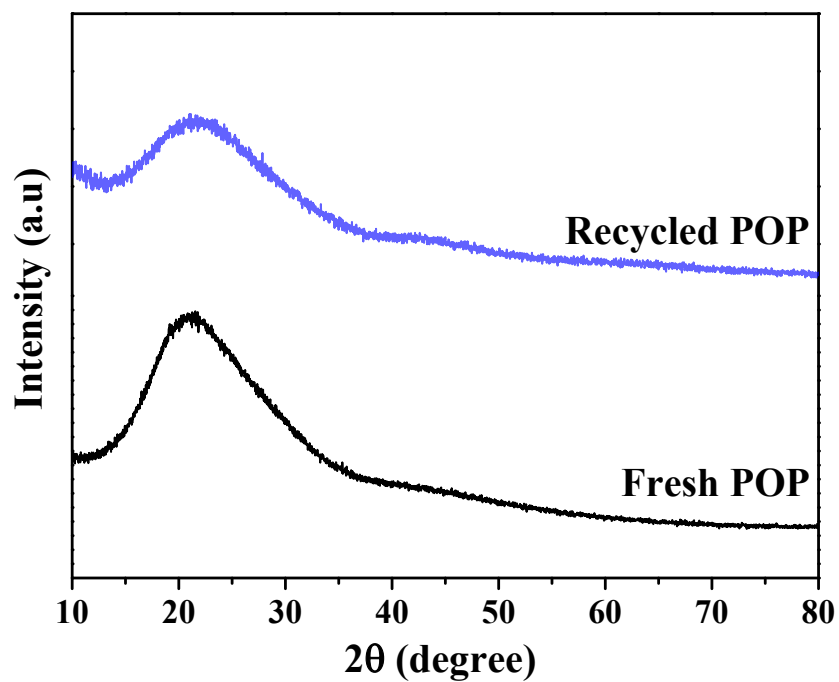


**Figure S2-** Powder X-ray diffraction (PXRD) patterns of the fresh and recycled POP.

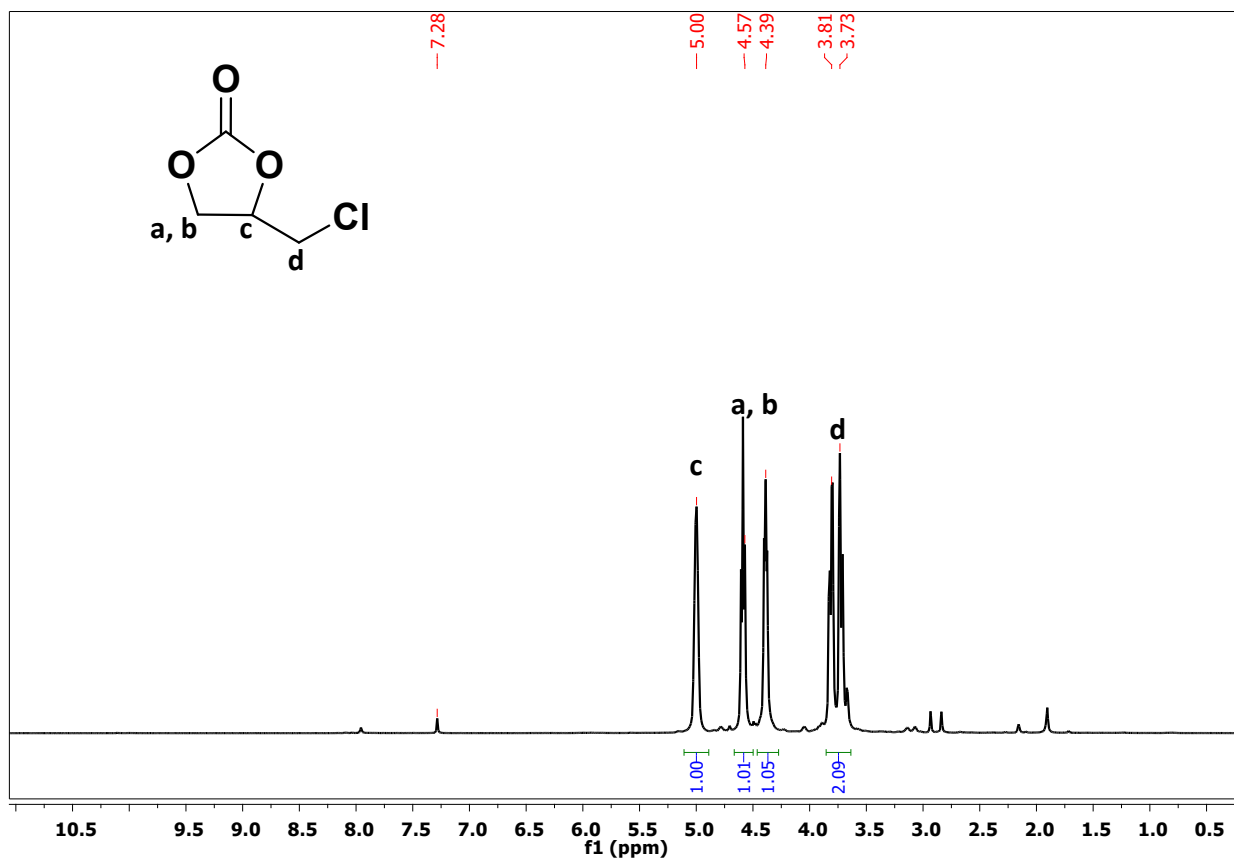


**Figure S3-**  $^1\text{H}$  NMR ( $\text{CDCl}_3$ , 500 MHz) spectrum of the 4-(chloromethyl)-1,3-dioxolan-2-one.

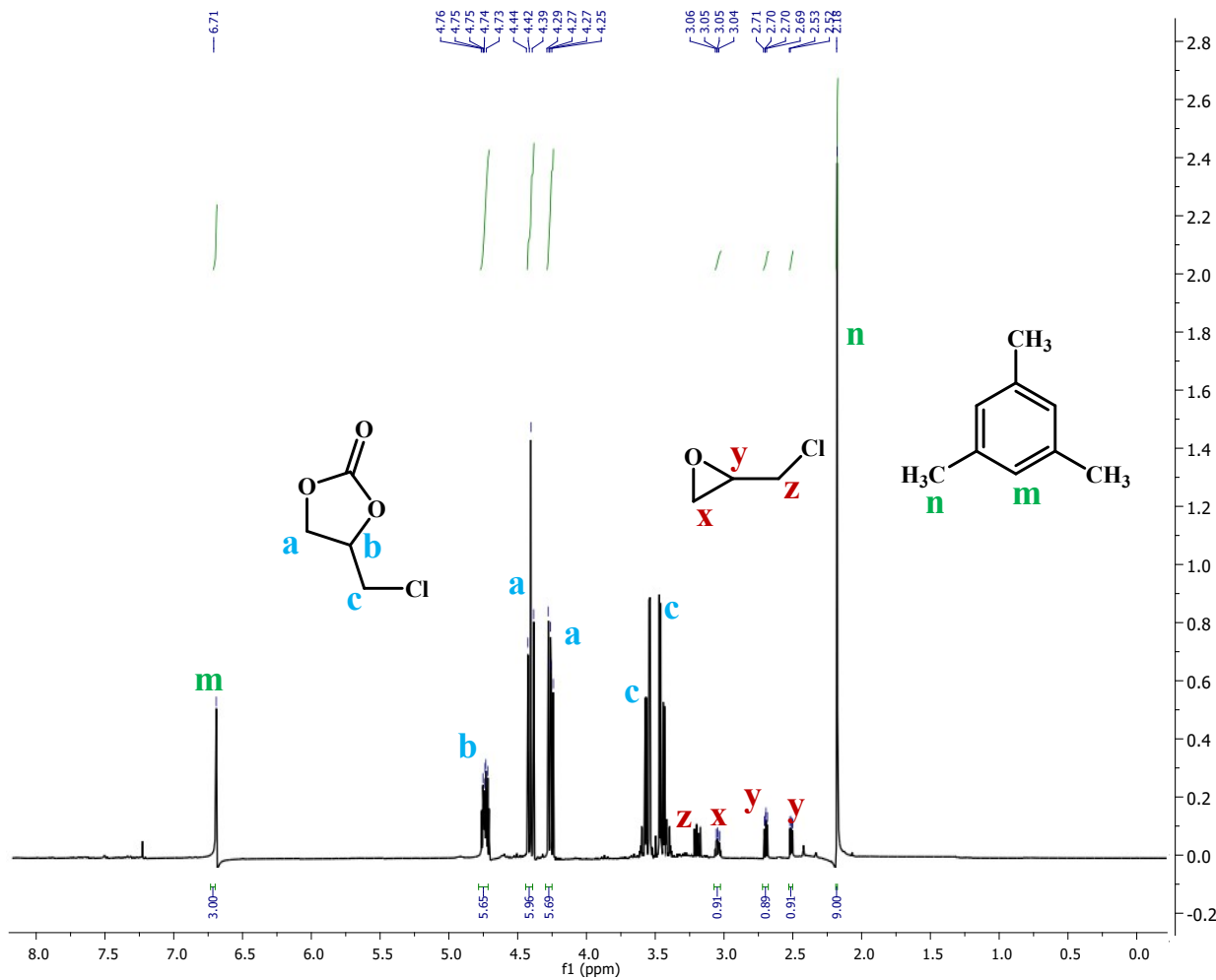


**Figure S4.**  ${}^1\text{H}$  NMR ( $\text{CDCl}_3$ , 500 MHz) spectrum for the cycloaddition reaction of epichlorohydrin with  $\text{CO}_2$  using POP. Mesitylene was used as an internal standard. Carbon balance for this reaction is found to be 98.1%.

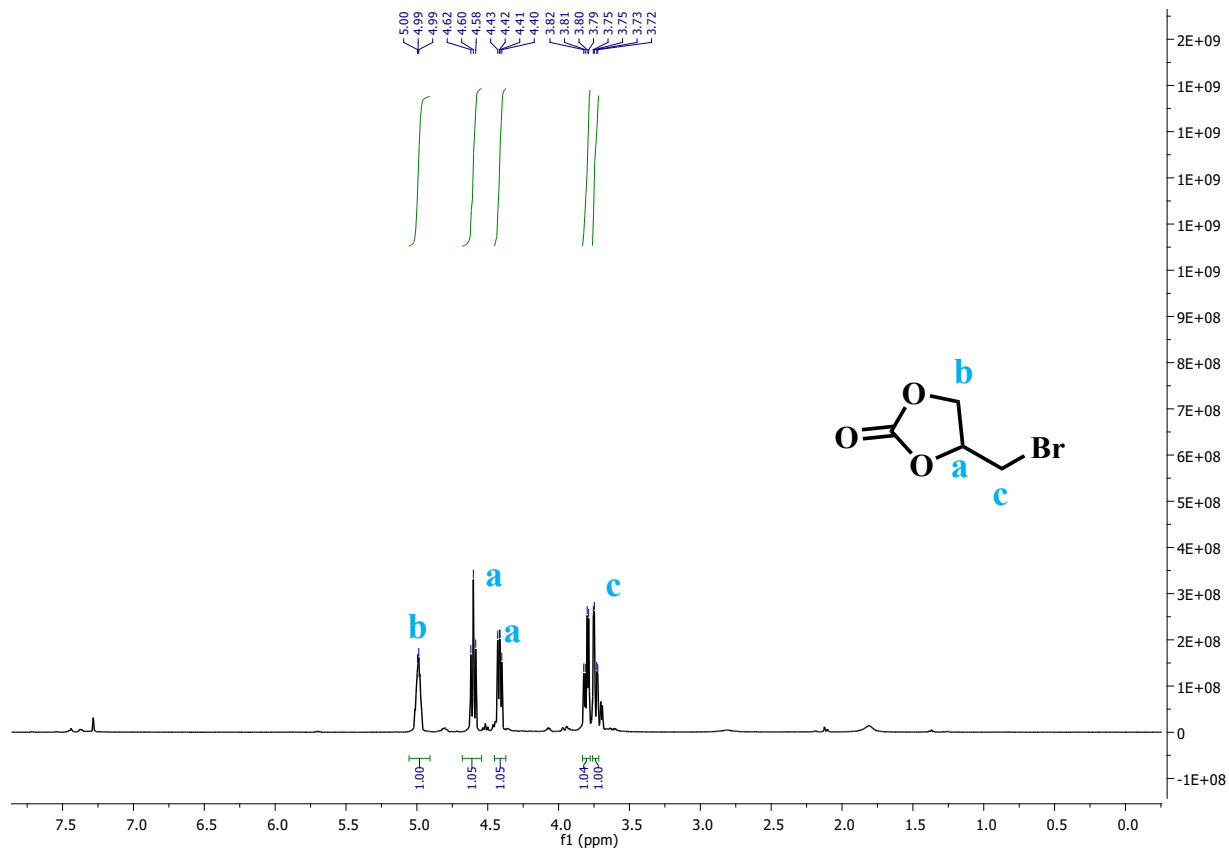


**Figure S5-**  $^1\text{H}$  NMR ( $\text{CDCl}_3$ , 500 MHz) spectrum of the 4-(bromomethyl)-1,3-dioxolan-2-one.

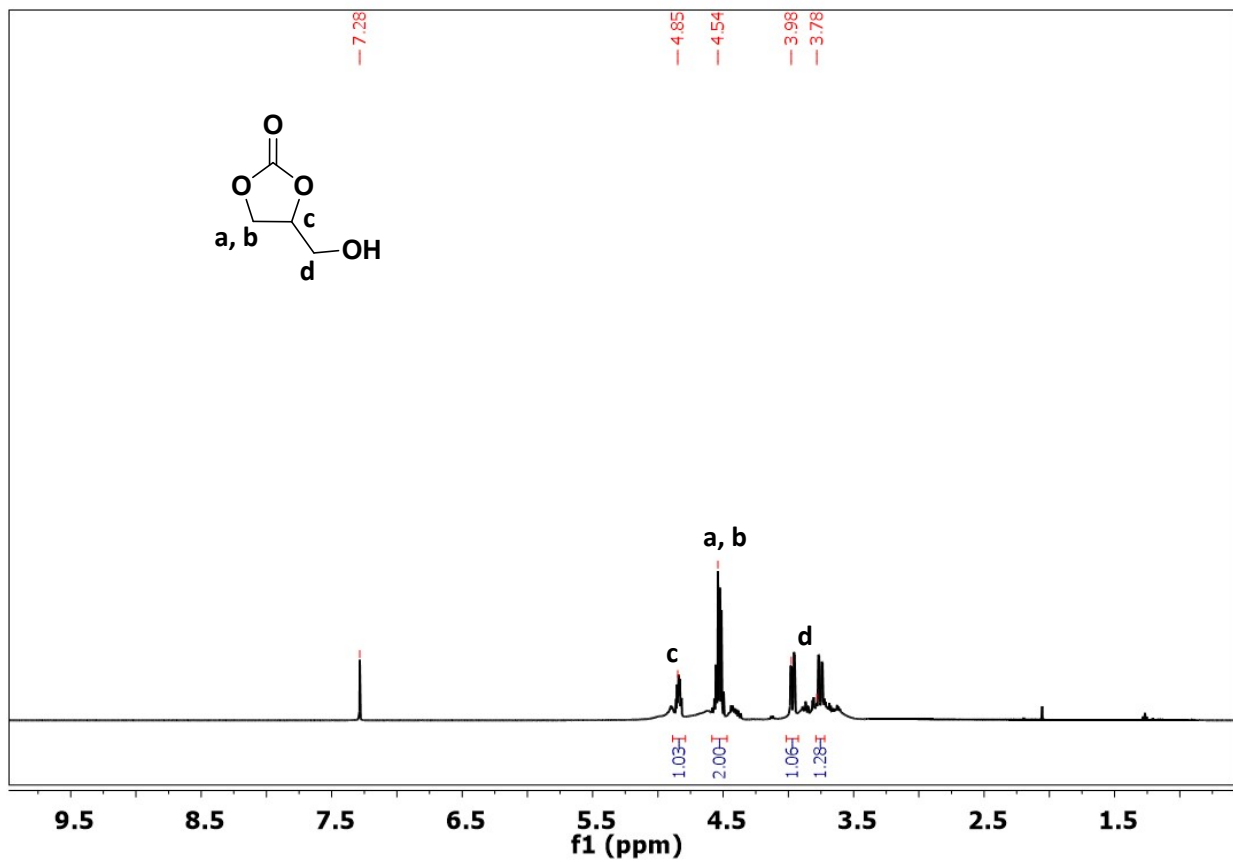


**Figure S6:** Reaction mixture consisting of Glycidol, glycerol carbonate and side products like glycerine and polyethers. The side products are detected by GC-MS.

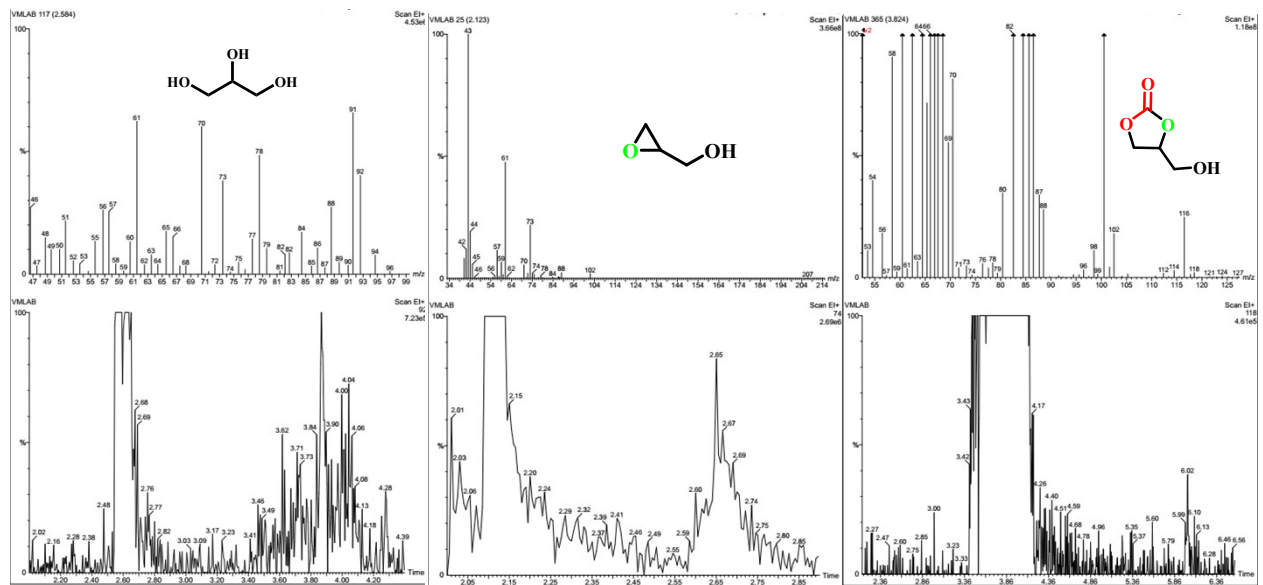


**Figure S7:** GC-MS spectra of the reaction mixture showing the presence of side products like glycerine.

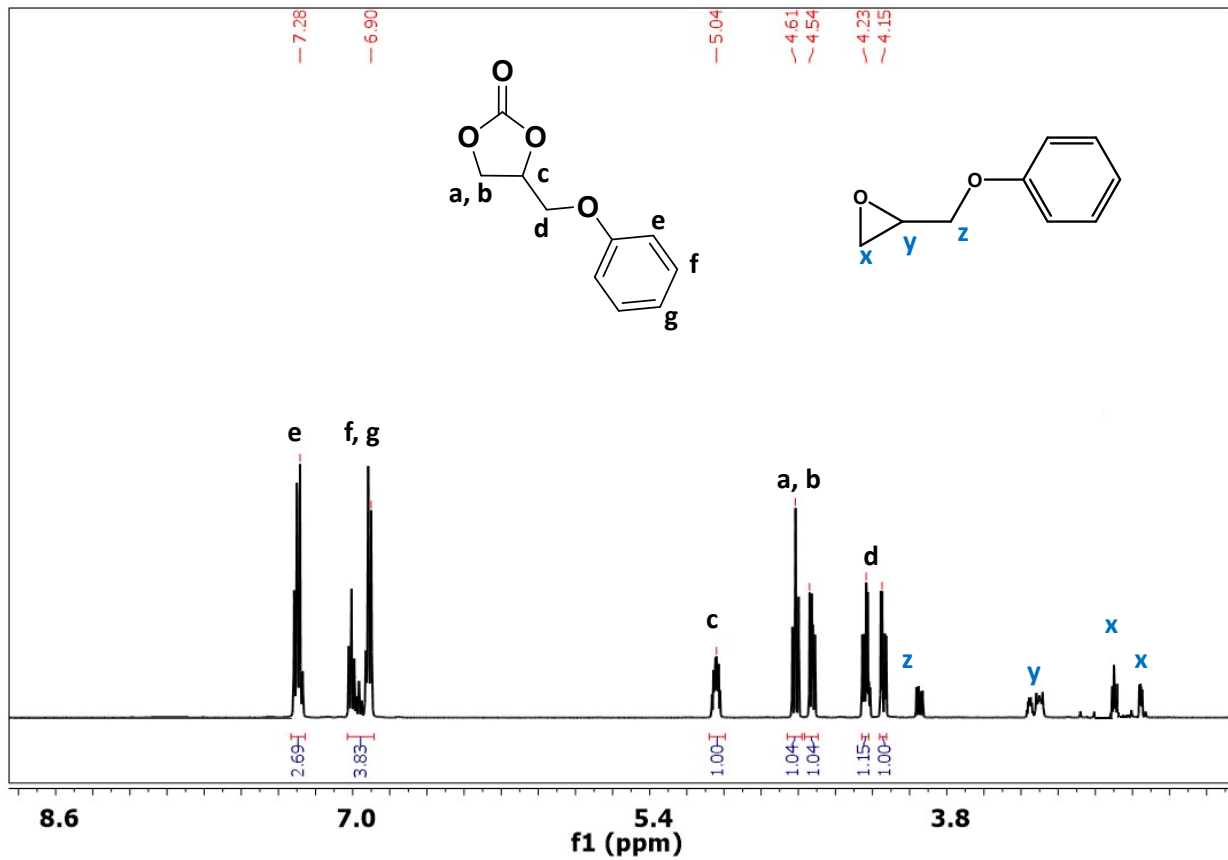


**Figure S8-**  $^1\text{H}$ -NMR of reaction mixture consisting of 4-(phenoxy methyl)-1,3-dioxolan-2-one ( $\text{CDCl}_3$ , 500 MHz) and phenyl glycidyl ether (90% conversion,  $130^\circ\text{C}$ )

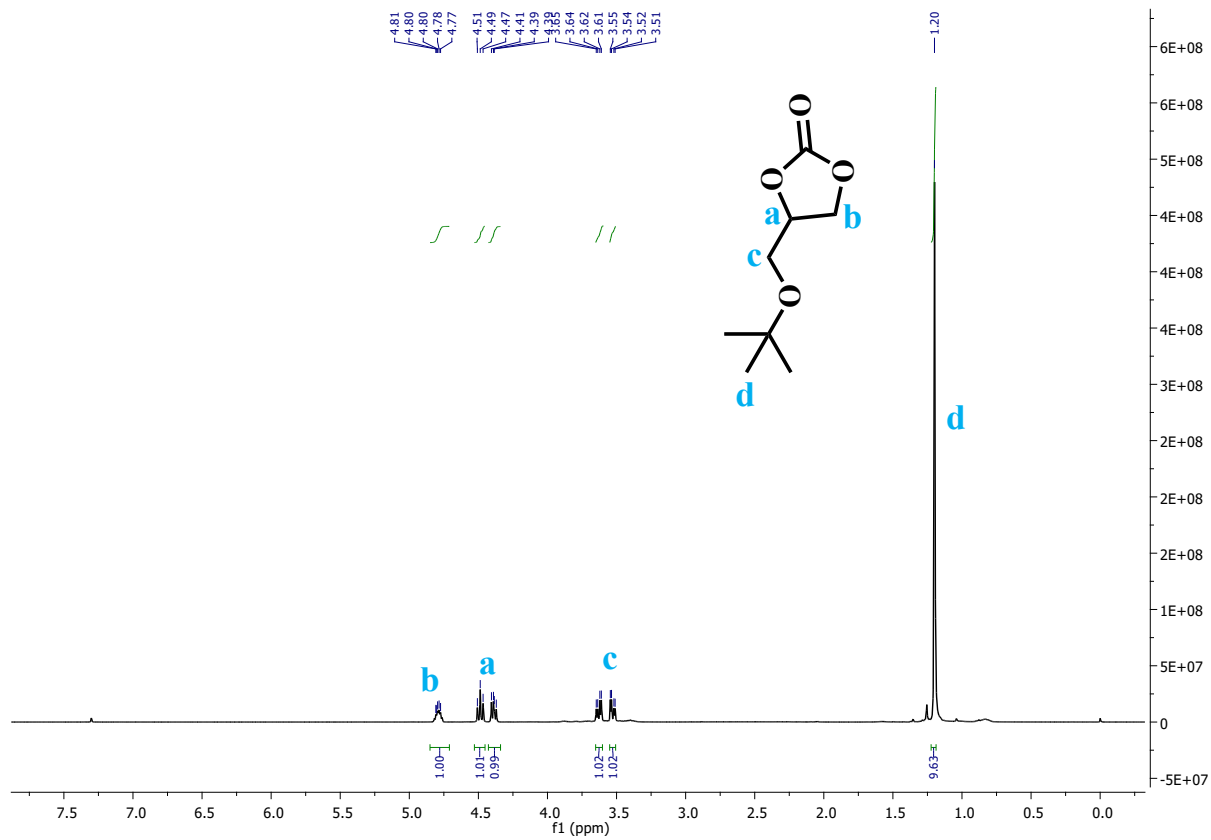


**Figure S9-**  $^1\text{H}$  NMR ( $\text{CDCl}_3$ , 500 MHz) spectrum of the 4-(tert-butoxymethyl)-1,3-dioxolan-2-one.

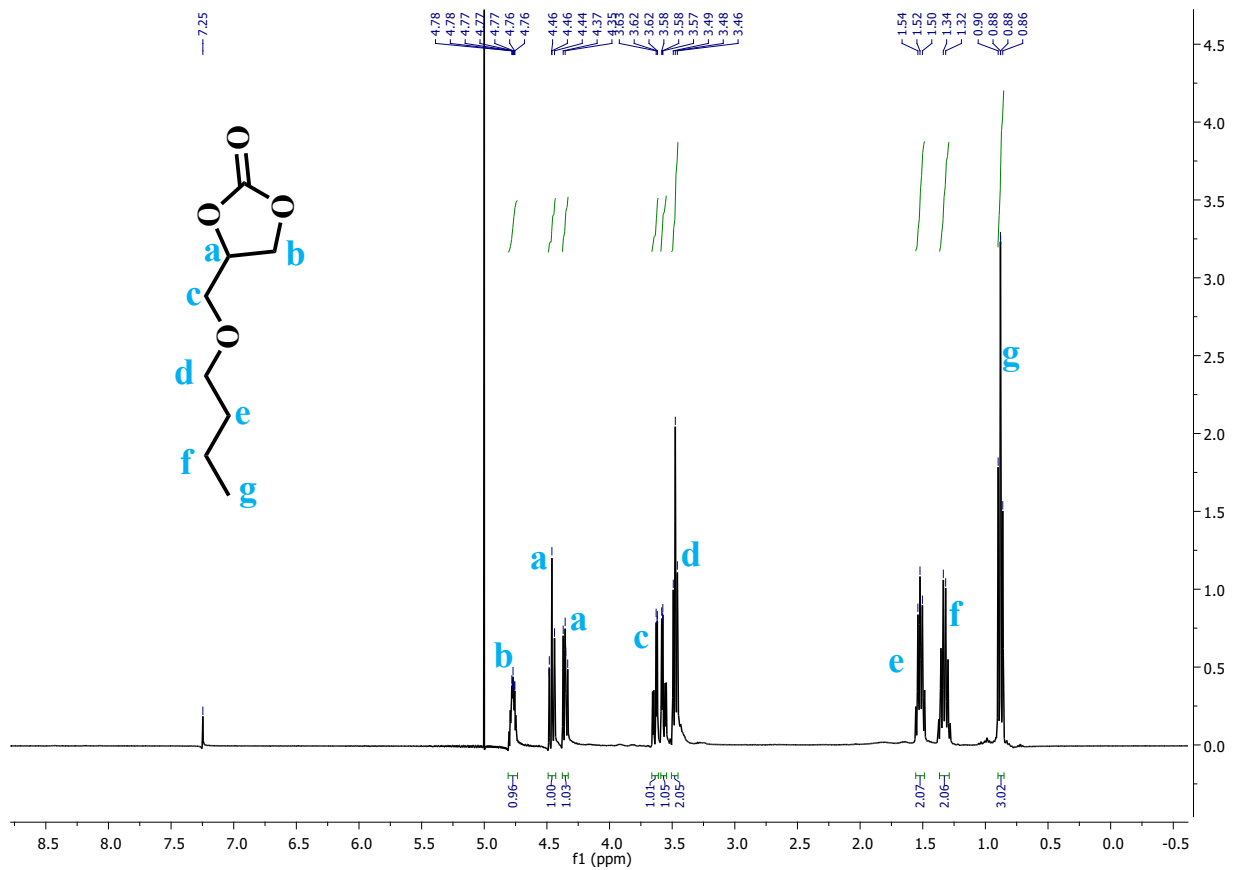


**Figure S10-**  $^1\text{H}$  NMR ( $\text{CDCl}_3$ , 500 MHz) spectrum of the 4-(n-butoxymethyl)-1,3-dioxolan-2-one.

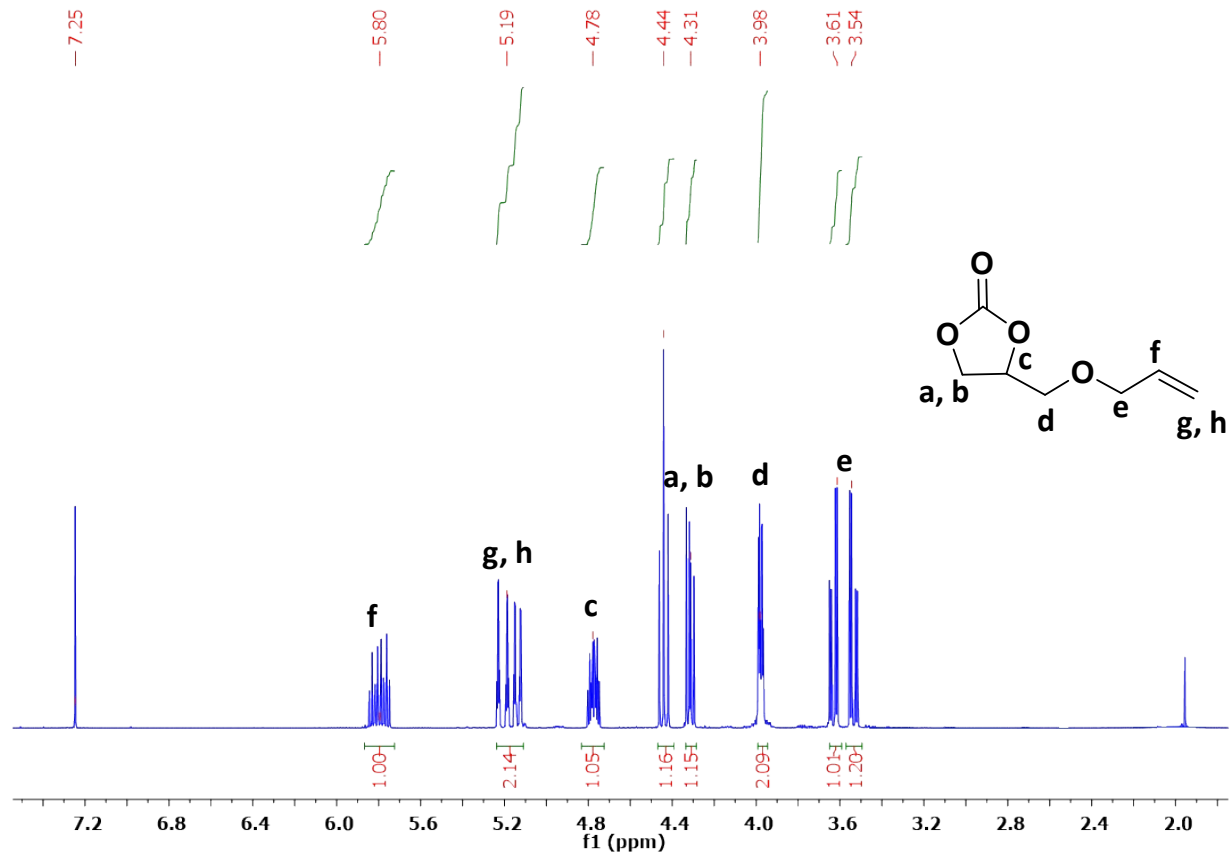


**Figure S11-**  $^1\text{H}$  NMR ( $\text{CDCl}_3$ , 500 MHz) spectrum of the 4-((allyloxy)methyl)-1,3-dioxolan-2-one.

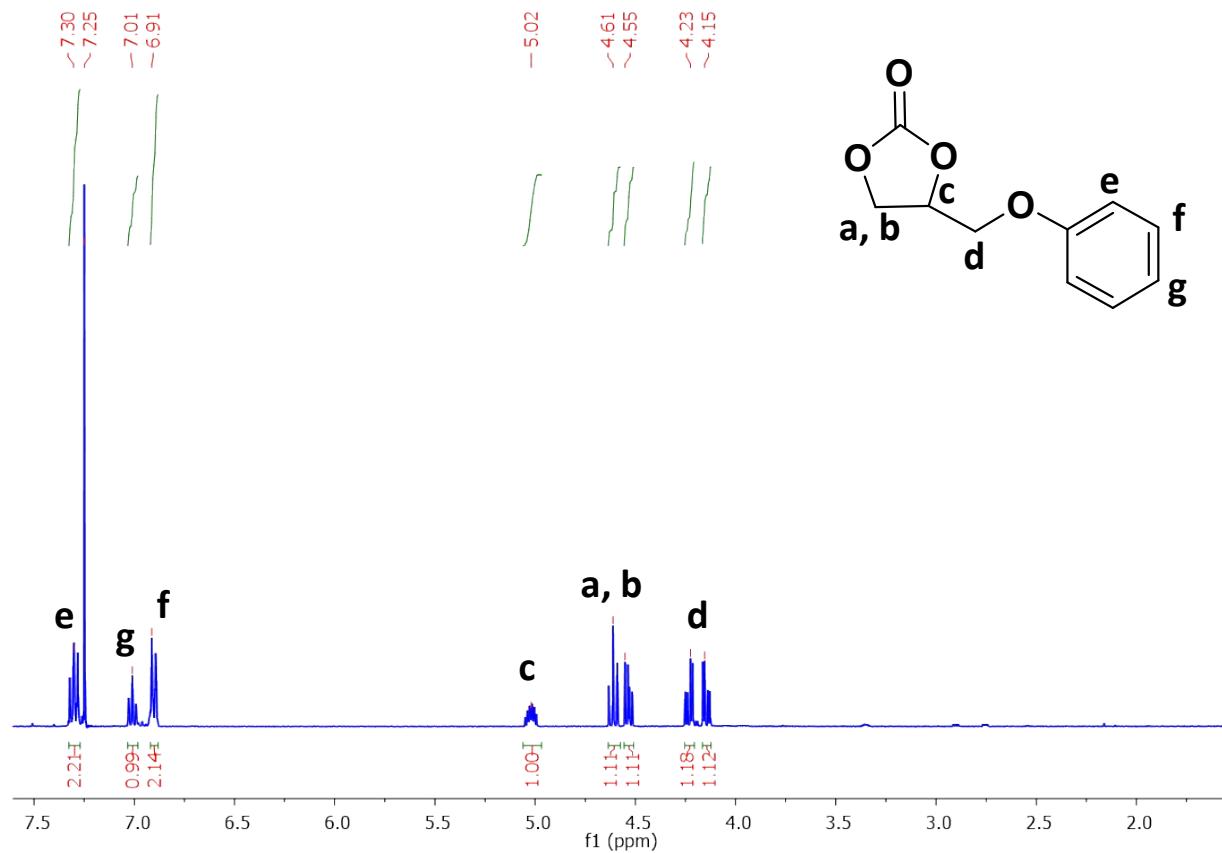


**Figure S12-**  $^1\text{H}$  NMR ( $\text{CDCl}_3$ , 500 MHz) spectrum of the 4-(phenoxy)methyl-1,3-dioxolan-2-one.

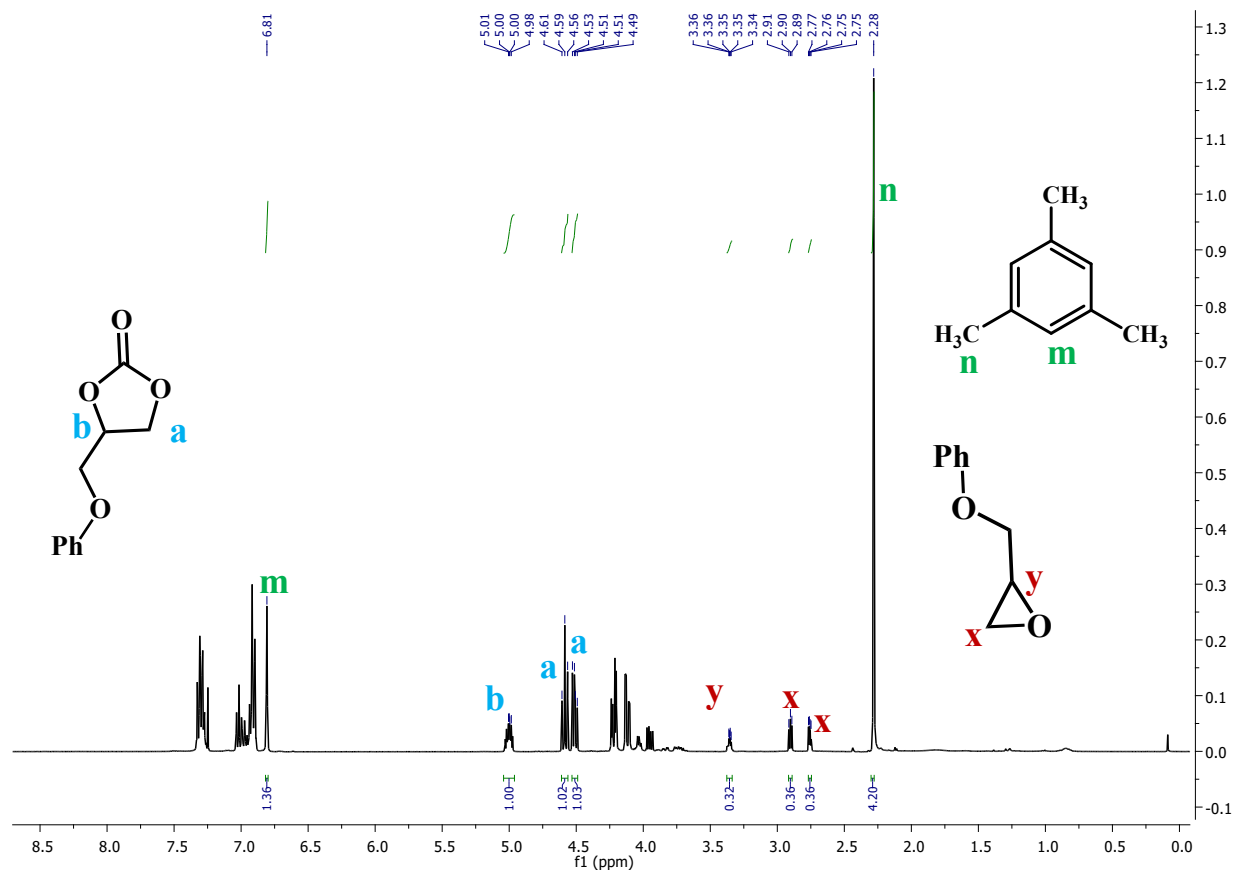


**Figure S13.**  $^1\text{H}$  NMR ( $\text{CDCl}_3$ , 500 MHz) spectrum for the cycloaddition reaction of 2-(phenoxy)methyl)oxirane with  $\text{CO}_2$  using POP. Mesitylene was used as an internal standard. Carbon balance for this reaction is found to be 100%.

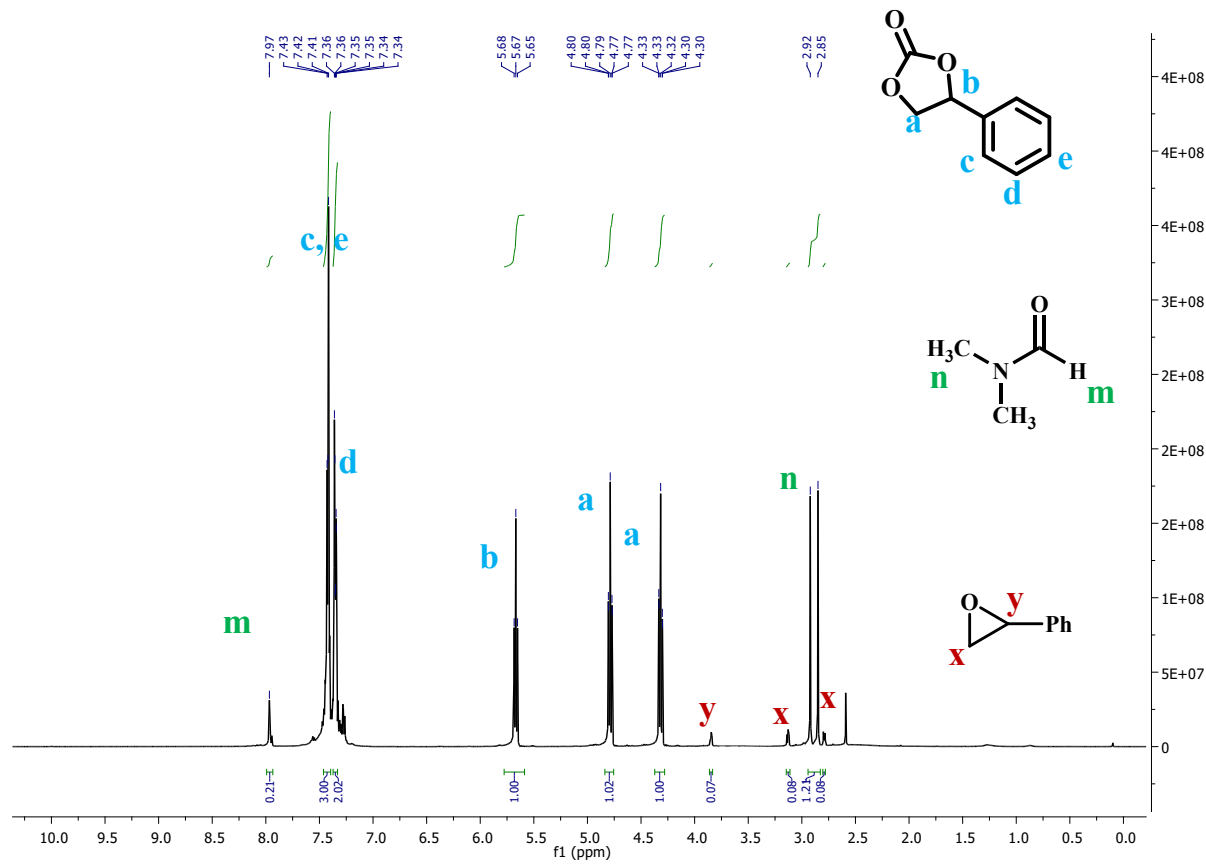


**Figure S14.**  $^1\text{H}$  NMR ( $\text{CDCl}_3$ , 500 MHz) spectrum for the cycloaddition reaction of 2-phenyloxirane with  $\text{CO}_2$  using POP and DMF (0.3 mmol).

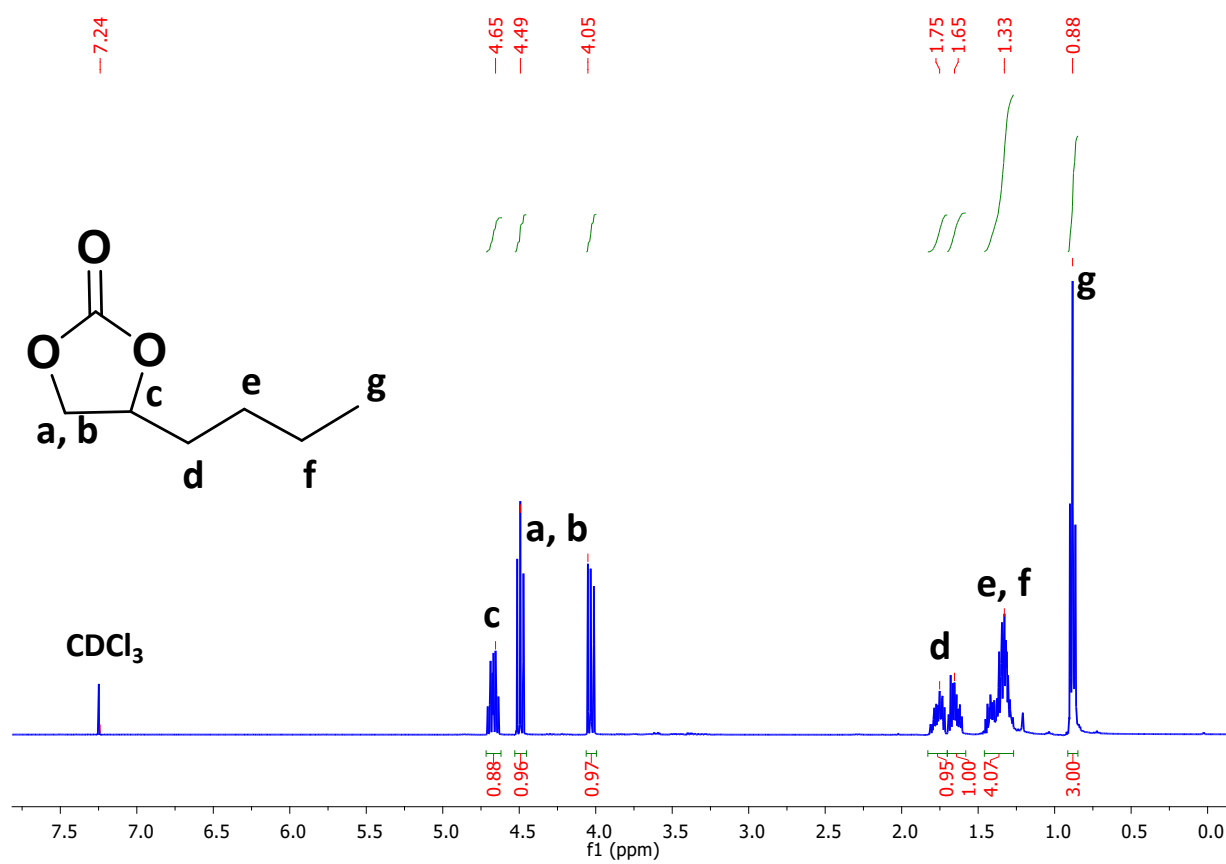


**Figure S15.**  $^1\text{H}$  NMR ( $\text{CDCl}_3$ , 500 MHz) spectrum of the 4-butyl-1,3-dioxolan-2-one.

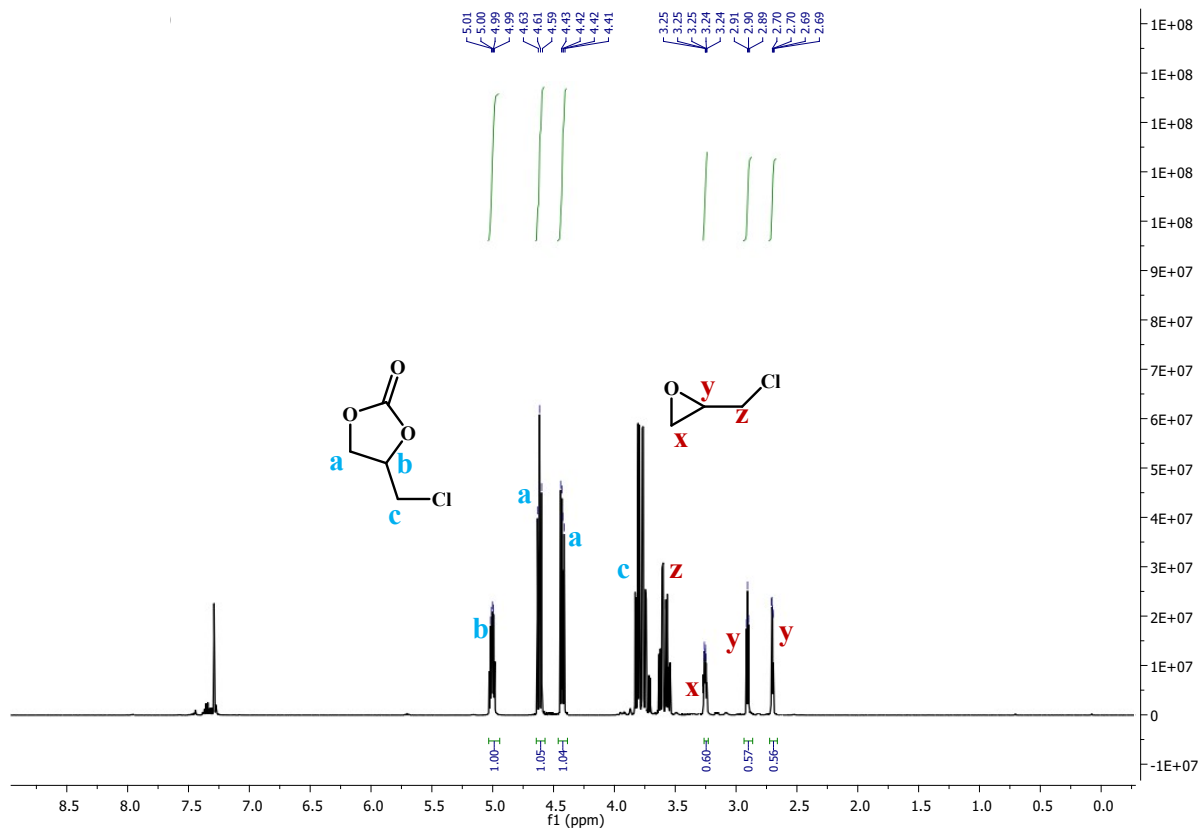


**Figure S16.**  $^1\text{H}$ -NMR spectrum of the reaction mixture after sixth cycle of catalysis. The mixture contains epichlorohydrin and 4- (chloromethyl)-1,3-dioxolan-2-one (64% conversion,  $\text{CDCl}_3$ )

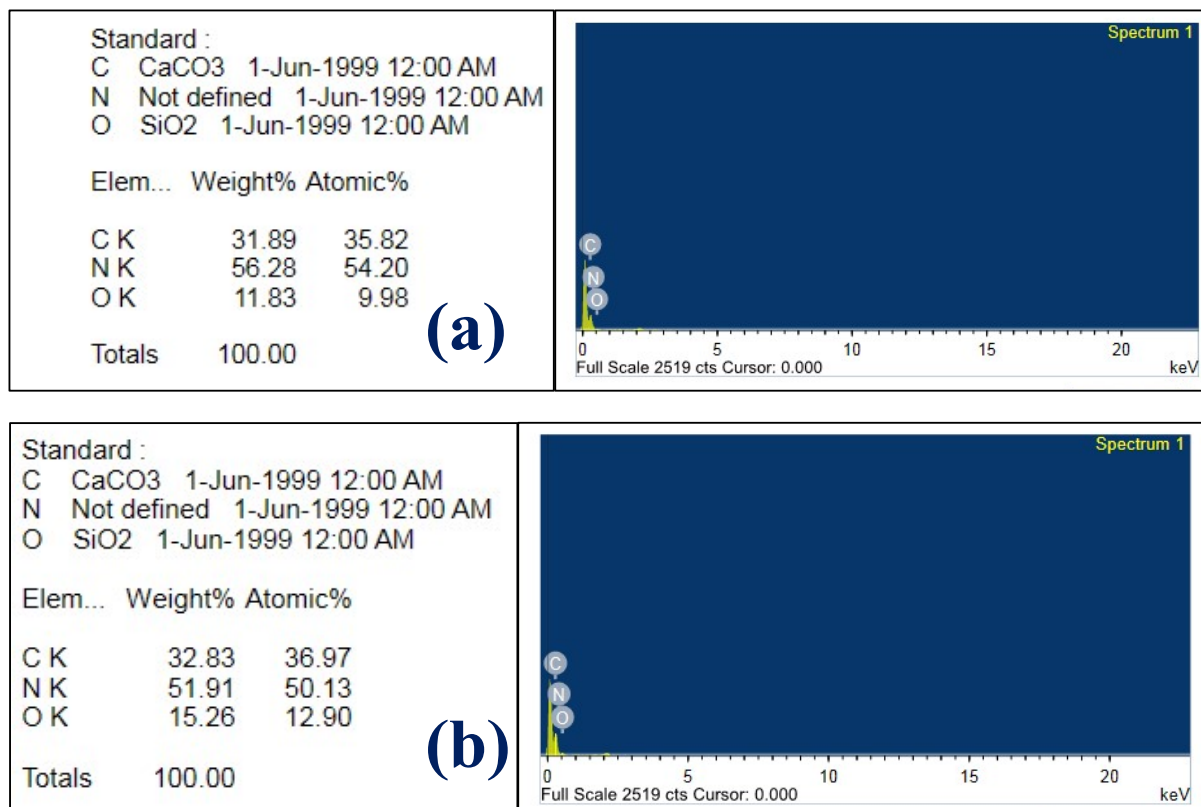


**Figure S17.** EDS spectrum of (a) fresh catalyst; (b) catalyst recovered after five catalytic cycles.

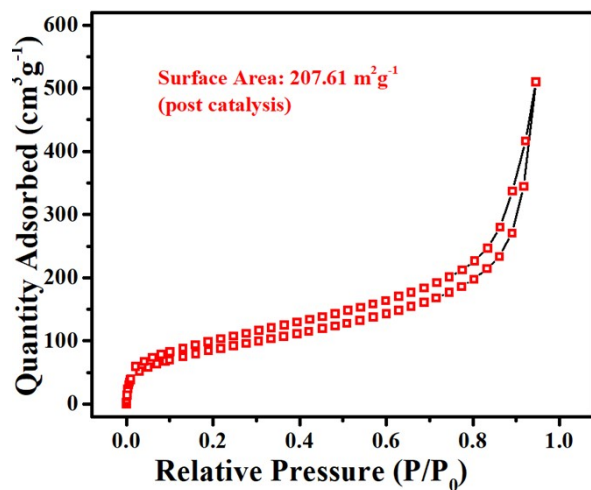


**Figure S18.** N<sub>2</sub> gas adsorption–desorption isotherm plot of POP obtained after 5<sup>th</sup> cycle of recyclability experiment.

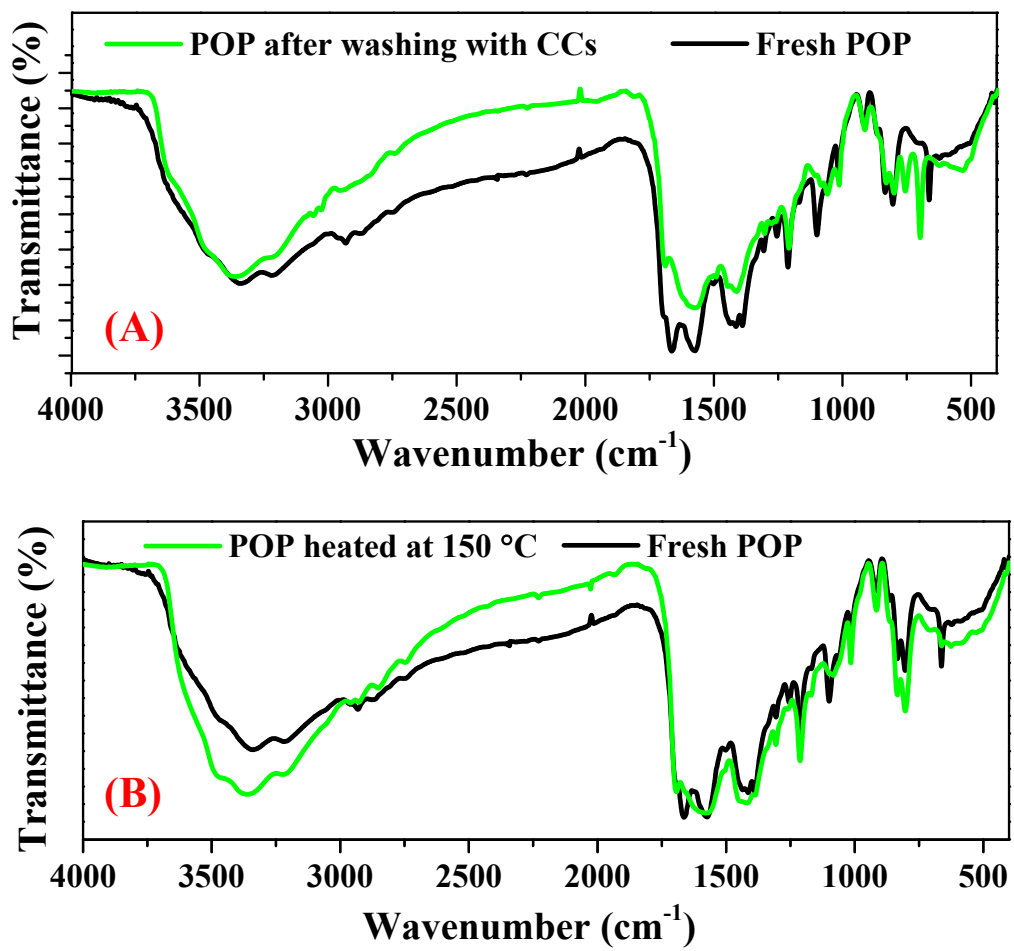


**Figure S19.** Comparison of FT-IR spectra. (a) as-prepared POP and recycled POP; (b) as-prepared POP and after heating it at 150 °C.

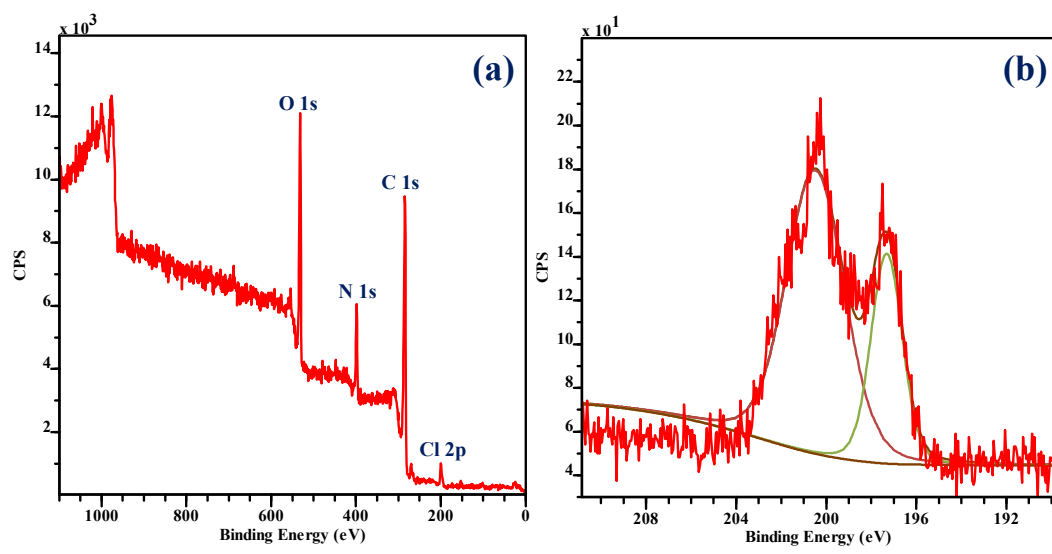


**Figure S20.** XPS of recycled catalyst **(a)** Survey scan showing the presence of chlorine which was absent in pre-catalyst; **(b)** Deconvoluted 2p Cl spectrum in the recycled catalyst (Chlorine content: 1.2%)

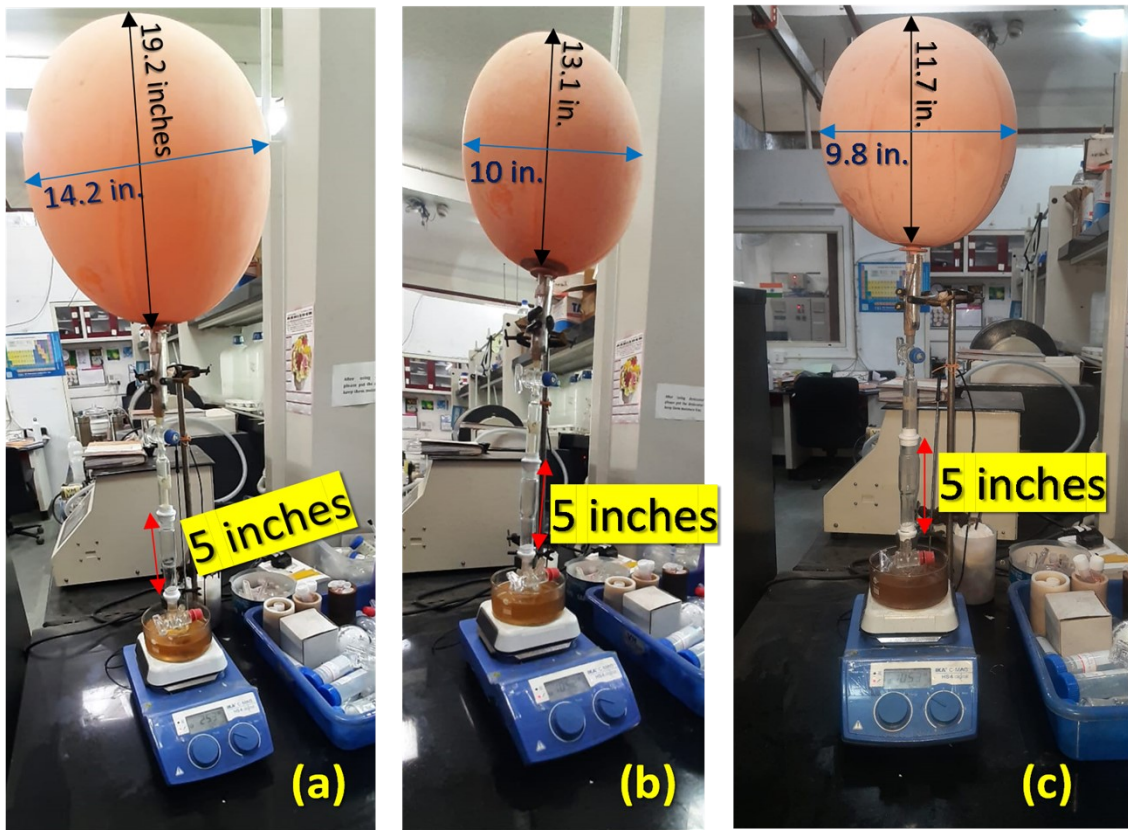


**Figure S21:** Digital image of the reaction setup showing the shrinking of the balloon through the course of reaction: (a) Start of the reaction; (b) after 12 hours; (c) After completion of the reaction (24 hours)

## References

- S1 Y. M. Li, L. Yang, L. Sun, L. Ma, W. Q. Deng and Z. Li, *J. Mater. Chem. A*, 2019, **7**, 26071–26076.
- S2 Z. Yue, T. Hu, H. Su, W. Zhao, Y. Li, H. Zhao, Y. Liu, H. Zhang, L. Jiang, X. Tang, S. Shan and Y. Zhi, *Fuel*, 2022, **326**, 125007.
- S3 S. Motokicho, Y. Takenouchi, R. Satoh, H. Morikawa and H. Nakatani, *ACS Sustain. Chem. Eng.*, 2020, **8**, 4337–4340.
- S4 J. Roeser, K. Kailasam and A. Thomas, *ChemSusChem*, 2012, **5**, 1793 –1799.
- S5 N. Zanda, A. Sobolewska, E. Alza, A. W. Kleij and M. A. Pericàs, *ACS Sustain. Chem. Eng.*, 2021, **9**, 4391–4397.
- S6 R. Sharma, A. Bansal, C. N. Ramachandran and P. Mohanty, *Chem. Commun.*, 2019, **55**, 11607–11610.
- S7 S. Subramanian, J. Park, J. Byun, Y. Jung and C. T. Yavuz, *ACS Appl. Mater. Interfaces*, 2018, **10**, 9478–9484.
- S8 W. Natongchai, J. A. Luque-Urrutia, C. Phungpanya, M. Sola, V. DElia, A. Poater and H. Zipse, *Org. Chem. Front.*, 2021, **8**, 613 —627
- S9 H. He, Q. Q. Zhu, J. N. Zhao, H. Sun, J. Chen, C. P. Li and M. Du, *Chem.—Eur. J.*, 2019, **25**, 11474 —11480
- S10 A. Mitra, T. Biswas, S. Ghosh, G. Tudu, K. S. Paliwal, S. Ghosh and V. Mahalingam, *Sustain. Energy Fuels*, 2022, **6**, 420–429.
- S11 A. Mitra, K. S. Paliwal, S. Ghosh, S. Bag, A. Roy, A. Chandrasekar, V. Mahalingam, *Inorg. Chem. Front.* 2023, **10**, 6329–6338.